Redox-Triggered FTIR Difference Spectra of FAD in Aqueous Solution and Bound to Flavoproteins†

Georg Wille,*,‡ Michaela Ritter,§ Rudolf Friedemann,|| Werner Mäntele,§ and Gerhard Hübner‡

Institut für Biochemie, Martin-Luther-Universität Halle-Wittenberg, Kurt-Mothes-Strasse 3, 06120 Halle, Germany, Institut für Organische Chemie, Martin-Luther-Universität Halle-Wittenberg, Kurt-Mothes-Strasse 2, 06120 Halle, Germany, and Institut für Biophysik, J. W. Goethe-Universität Frankfurt/Main, Theodor-Stern-Kai 7, Haus 74, 60590 Frankfurt/Main, Germany

Received July 10, 2003; Revised Manuscript Received October 16, 2003

ABSTRACT: Flavin adenine dinucleotide (FAD) and three different flavoproteins in aqueous solution were subjected to redox-triggered Fourier transform infrared difference spectroscopy. The acquired vibrational spectra show a great number of positive and negative peaks, pertaining to the oxidized and reduced state of the molecule, respectively. Density functional theory calculations on the B3LYP/6-31G(d) level were employed to assign several of the observed bands to vibrational modes of the isoalloxazine moiety of the flavin cofactor in both its oxidized and, for the first time, its reduced state. Prominent modes measured for oxidized FAD include $\nu(C_4{=}O)$ and $\nu(C_2{=}O)$ at 1716 and 1674 cm^{-1}, respectively, $\nu(C_{4a}{=}N_5)$ at 1580 cm^{-1}, and $\nu(C_{10a}{=}N_1)$ at 1548 cm^{-1}. Measured modes of the reduced form of FAD include $\nu(C_2{=}O)$ at 1692 cm^{-1}, $\nu(C_4{=}O)$ at 1634 cm^{-1}, and $\nu(C_{4a}{=}C_{10a})$ at 1600 cm^{-1}. While the overall shape of the enzyme spectra is similar to the shape of the spectrum of free FAD, there are numerous differences in detail. In particular, the $\nu(C{=}N)$ modes of the flavin exhibit frequency shifts in the protein-bound form, most prominently for pyruvate oxidase where $\nu(C_{10a}{=}N_1)$ downshifts by 14 cm^{-1} to 1534 cm^{-1}. The significance of this shift and a possible explanation in connection with the bent conformation of the flavin cofactor in this enzyme are discussed.

The flavin derivatives FAD[1] and FMN are widespread as cofactors among enzymes that catalyze redox reactions. Figure 1 shows a schematic representation of the two-electron reduction of oxidized flavins. The molecular details of this process and the properties of the flavin moiety, such as its redox potential, UV−vis spectrum, reaction rate constants, etc., are strongly influenced by the protein environment of the cofactor.

The cycling between different states of oxidation is accompanied by a rearrangement of single and double bonds involving the $N_5-C_{4a}-C_{10a}-N_1$ atom group. These changes in the bonding pattern in the cofactor should be detectable, at least in theory, with vibrational spectroscopy, but the vastly larger number of bonds in the protein itself and the bulk solvent will dominate over any signal originating from the cofactor. Therefore, a method is needed to select the vibrational modes of the cofactor. One such method is resonance Raman spectroscopy, which has already been applied successfully to the investigation of flavoproteins (*1*, *2*). The flavin cofactors FAD and FMN lend themselves naturally to this method, as in the oxidized state they both exhibit strong electronic absorption bands that can be used to excite a resonance Raman spectrum. The disadvantage is that the reduced form of the flavin is only a weak Raman scatterer, limiting the investigation almost exclusively to the oxidized state or to complexes of the reduced enzyme with a compound that gives rise to an excitable electronic charge transfer band (*3*). Furthermore, resonance Raman spectroscopy will only report on the immediate vicinity of the cofactor, and not on protein reactions coupled to the cofactor.

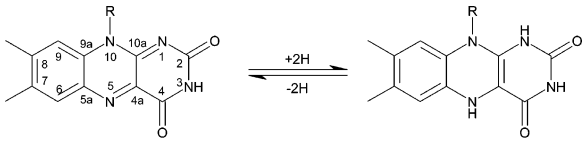

FIGURE 1: Structure and redox reaction of the active isoalloxazine moiety in flavin cofactors (pH 6.0). For lumiflavin, R is CH_3. For FMN, R is ribityl phosphate. For FAD, R is ribityl-ADP.

Another method for suppressing vibrational modes of the protein and solvent is to exploit the fact that most of them are independent of the redox state, while those of the cofactor and its vicinity are not. Thus, for the technique of electrochemically triggered FTIR difference spectroscopy, one applies a given redox potential to the chemical system in the IR cell, and collects an IR spectrum of the resulting state.

† This work was supported by the Deutsche Forschungsgemeinschaft and the Fonds der Chemischen Industrie.

* To whom correspondence should be addressed. E-mail: georg@bc.biochemtech.uni-halle.de. Phone: +49-345-5524835. Fax: +49-345-5527014.

‡ Institut für Biochemie, Martin-Luther-Universität Halle-Wittenberg.

§ J. W. Goethe-Universität Frankfurt/Main.

|| Institut für Organische Chemie, Martin-Luther-Universität Halle-Wittenberg.

[1] Abbreviations: FAD, flavin adenine dinucleotide; FMN, flavin mononucleotide; UV−vis, ultraviolet−visible light; IR, infrared; FTIR, Fourier transform infrared; POX, pyruvate oxidase; GOX, glucose oxidase; DAO, D-amino acid oxidase; DFT, density functional theory; ThDP, thiamin diphosphate; ADP, adenosine diphosphate; fwhh, full width at half-height.

10.1021/bi035219f CCC: $25.00
Published on Web 11/26/2003

This procedure is then repeated at a different redox potential, and the two spectra are subtracted. Because of the high precision that can be attained, the entire spectral contribution that does not change upon reduction or oxidation can be filtered out; the great majority of bands of both the protein and solvent water disappear from the difference spectrum of the two states of the system. Therefore, while a single IR spectrum of an aqueous protein solution shows only "low-resolution" features such as the prominent broad amide bands, the difference spectrum of two different redox states reveals a number of highly detailed features pertaining to a chemical process (*4*, *5*).

In this study, we set out to apply this method to FAD both in aqueous solution and bound to three different flavoenzymes. All three enzymes, pyruvate oxidase from *Lactobacillus plantarum* (POX), glucose oxidase from *Aspergillus niger* (GOX), and porcine D-amino acid oxidase (DAO), catalyze the two-electron oxidation of their respective substrates in a manner concomitant with the reduction of bound FAD, which is then reoxidized by molecular oxygen to yield hydrogen peroxide. In this group of enzymes, POX is special with respect to its mode of flavin binding. Here, the isoalloxazine moiety deviates from planarity by a bend about the N_5-N_{10} axis of 13° (*6*), whereas the available crystal structures indicate a planar conformation of the cofactor in GOX (PDB entry 1CF3) and a slight bend of ~6° in DAO (PDB entry 1AA8), with some uncertainty due to a resolution of only 2.5 Å in the latter case. The aims of this study were thus twofold. We wanted to compare the IR difference spectra of FAD in solution and bound to protein, as well as spectra of FAD bound to different proteins, to see whether the strained binding of the cofactor in POX is reflected in the IR spectrum.

For a more detailed interpretation of the obtained difference spectra, we attempted to assign observed peaks to vibrational modes of the molecule. Because of the large number of possible modes (generally $3N - 6$ modes in a molecule of N atoms) and extensive coupling of atomic motions, an *a priori* assignment of peaks in an IR spectrum to specific vibrational modes is notoriously difficult. In the case of flavins, additional information is available in the form of studies with isotopically labeled flavin derivatives (*7*, *8*), as well as theoretical normal-mode calculations (*9*−*11*). However, this additional information, in particular, the normal-mode calculations, almost exclusively pertains to the oxidized species, presumably because hardly any vibrational spectra of the reduced species are available for reference. We are aware of only one study by Birss et al. presenting an IR spectrum of the anionic reduced form of FAD (*12*), also obtained through electrochemical methods. However, the band assignment given there is largely empirical. Therefore, we performed frequency calculations with the DFT method for both the fully reduced and the oxidized state of the model compound lumiflavin (C_7,C_8,N_{10}-trimethylisoalloxazine) to obtain estimates for mode frequencies and intensities and thus to assign experimentally observed bands.

MATERIALS AND METHODS

Glucose oxidase from *A. niger*, porcine kidney D-amino acid oxidase, thiamin, ThDP, and FMN were purchased from Sigma Aldrich. FAD was from AppliChem. Commercially available enzymes and substances were used without further purification.

Protein Expression and Purification. Pyruvate oxidase was expressed recombinantly in *Escherichia coli* strain C600, carrying the pBP200 plasmid with the *pox* gene of *L. plantarum* under the control of a tac promoter and conferring ampicillin resistance. The plasmid was a kind gift from R. Rudolph. The *E. coli* strain furthermore carried the pFDX500Δdra plasmid with the *lacI*^{Q} gene for the lac repressor to reduce the level of background expression, and conferring kanamycin resistance. This plasmid was kindly provided by J. Winter.

A medium (4.2 L) containing 10 g/L peptone, 5 g/L yeast extract, 15 g/L lactose, 100 mg/L ampicillin, 50 mg/L kanamycin, 35 mg/L thiamin, 50 mg/L FMN, and 100 mM potassium dihydrogen phosphate was inoculated from an overnight culture of cells in the same medium without lactose. Bacterial growth and protein expression continued for 15 h at 30 °C with constant shaking. Cells were harvested by centrifugation and disrupted by two freeze−thaw cycles followed by addition of an equal volume of 50 mM potassium phosphate buffer (pH 6.0), 10% (v/v) glycerol, 1 mM ThDP, 1 mM $MgSO_4$, and 1 mM FAD, and subsequent French press lysis. Protamine sulfate was added to the lysate to a final concentration of 0.5% (w/v). Cellular debris and precipitated nucleic acids were removed by ultracentrifugation at 50000*g* for 30 min. The cleared cell extract was then submitted to a fractionated ammonium sulfate precipitation between 23 and 33% (w/v). The resulting pellet was dissolved in 1 mL of glycerol and 3 mL of buffer containing 20 mM potassium phosphate (pH 6.0), 100 μM ThDP, and 100 μM $MgSO_4$. The clear dark yellow solution was then dialyzed overnight against 1 L of the same buffer without glycerol. The resulting precipitate was removed by centrifugation, and the protein solution was applied to a Source 15Q anion exchange column (Pharmacia) equilibrated with dialysis buffer. Elution was achieved by a gradient of dialysis buffer with an increasing concentration of potassium phosphate (pH 6.0). Yellow fractions were collected and analyzed by SDS gel electrophoresis. Sufficiently pure fractions were combined and concentrated by ammonium sulfate precipitation with 40% (w/v) ammonium sulfate. The pellet was dissolved in the smallest possible volume of a 200 mM potassium phosphate buffer (pH 6.0). The solution was cleared by centrifugation and applied to a 120 mL Superdex 200 prep grade gel filtration column (Pharmacia). The protein was eluted with the same buffer. Yellow fractions were collected, checked for purity by SDS gel electrophoresis, combined, and concentrated using Macrosep (Pall) centrifugation devices. After addition of 10% (v/v) glycerol, the sample was divided into aliquots and stored frozen at −80 °C. POX apoenzyme was obtained according to the method of Sedewitz (*13*).

Sample Preparation. Protein samples for spectroelectrochemistry were prepared by buffer exchange and concentrating the protein solution to ~1−3 mM bound FAD (i.e., active sites) using Microcon (Amicon) centrifugation devices. The buffers used for the protein solutions were as follows: 100 mM potassium phosphate (pH 6.0) and 50 mM potassium chloride for POX, 100 mM potassium phosphate (pH 6.5) and 100 mM potassium chloride for GOX, and 100 mM potassium pyrophosphate (pH 8.3) and 100 mM potassium

chloride for DAO. In all cases, the final flow-through of the centrifugation devices was clear buffer, in contrast to the brightly yellow protein solution, indicating that all FAD was bound to protein. FAD spectra were obtained with a 10 mM solution in 100 mM potassium phosphate (pH 6.0) and 100 mM potassium chloride.

Electrochemistry. The electrochemical IR cell was used as previously described (*4*). The surface of the gold grid working electrode was chemically modified with a 2 mM cysteamine solution. A mix of redox mediators was added to the protein solution prior to its application to the cell to accelerate the redox reaction (for the composition, see ref *14*, except diethyl-3-methylparaphenylenediamine and dimethylparaphenylenediamine, but adding quinhydrone; final concentration of each component of ~40 μM). The cell was then filled with 6−10 μL of a protein solution and the path length adjusted to 6−8 μm. The temperature of the sample cell was kept at 15 °C during measurements. Quoted electrochemical potentials refer to an Ag/AgCl/3 M KCl reference electrode; for potentials against the standard hydrogen electrode, 208 mV should be added.

Spectroscopy. A modified IFS 25 FTIR spectrometer (Bruker) was used for the simultaneous acquisition of IR spectra between 2000 and 1000 cm^{-1} and visible spectra between 400 and 800 nm as a function of the redox potential in the cell. The sample was equilibrated with an initial potential at the working electrode, and a single beam spectrum was obtained. The potential then was changed to its final value and the sample allowed to reequilibrate. Completion of this process was checked by monitoring the electrode current and successive IR spectra until no further change was found. A second spectrum was then measured, and the difference spectrum was calculated with the initial spectrum as a reference. For acquisition of IR spectra, 128 interferograms at 4 cm^{-1} resolution were added and Fourier transformed using triangular apodization and a zero filling factor of 2.

If appropriate, spectra were corrected for baseline drift. The baseline was established by averaging two subsequent difference spectra, obtained after redox transitions in opposite directions. This average spectrum, in which all redox-dependent contributions are canceled out, assumes the shape of an IR spectrum of an aqueous protein solution and reflects miniscule changes in the thickness of the liquid layer in the IR cell.

Density Functional Theory Calculations. For a tentative assignment of bands in the IR difference spectra to vibrational modes of the flavin cofactor, frequency calculations on the B3LYP/6-31G(d) level were carried out for the model compound lumiflavin in its oxidized and two-electron-reduced states (Figure 1), assuming a *T* of 298 K and a *p* of 1 atm. First, an optimization procedure was performed to obtain the energetically preferred structure of the molecule. Structures with minimal energy were characterized by computing their vibrational spectrum and identified by the absence of imaginary frequencies. These calculations were carried out on a Silicon Graphics workstation using the program package Gaussian 98 and GaussView, version 2 (*15*). The obtained frequencies were scaled by a single scale factor of 0.9614 according to ref *16*, which showed that this empirical correction results in a list of frequencies of which ~86% deviate less than 6% from the measured value in a test set of molecules. The root-mean-square deviation is given as 34 cm^{-1}.

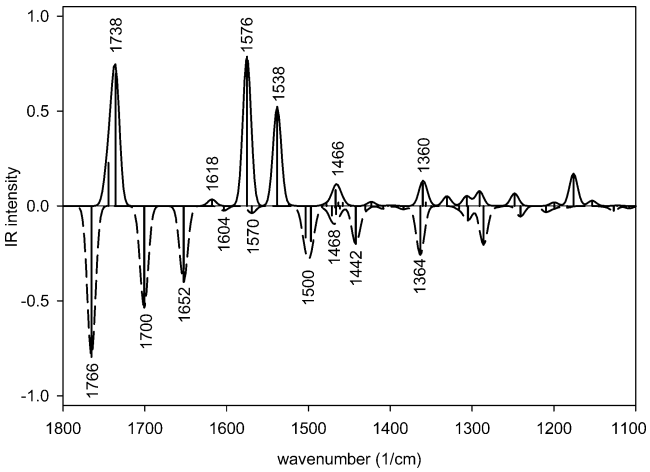

FIGURE 2: Calculated IR spectra of lumiflavin in the oxidized (—) and reduced state (− − −). IR intensity is in arbitrary units. The vertical bars give the frequency and intensity of all modes contributing to the spectra; in some cases, a peak derives from more than one mode. All peaks were generated from the bars by expanding them into a Gaussian profile with a fwhh of 7 cm^{-1}.

From the list of frequencies and intensities, the IR spectrum was simulated by expanding each line into a Gaussian peak with a full width at half-height of 7 cm^{-1}, as estimated from the measured spectra.

RESULTS AND DISCUSSION

With respect to all measured spectra given below, both for the free FAD and for the flavoproteins, we note that visible light difference spectra acquired simultaneously from the same samples (data not shown) gave no indication of the presence of red or blue radical semiquinone species, which are well-known for flavin chemistry. This allows us to neglect contributions of these radicals to the vibrational spectra and to limit the discussion to the fully oxidized and reduced species.

Energy minimization and normal-mode analyses for both the reduced and the oxidized form of model compound lumiflavin were performed to obtain theoretical spectra. These calculations show that the preferred structure for the oxidized compound is planar, whereas the most stable conformation of the reduced form deviates from planarity by a 26° bend about the N_5-N_{10} axis. This is in very good agreement with earlier work by Zheng et al. and Rizzo et al. (*17*, *18*). Several simplifications were made to keep the system computationally tractable. The effects of hydrogen bonding at N_1, N_3, N_5, and the two carbonyl groups have generally been omitted, except for one case of a lumiflavin monohydrate described below. Furthermore, the model compound lumiflavin lacks the ribityl-ADP moiety, which in the case of FAD is linked to N_{10} of the isoalloxazine ring, so that any influence of this residue on the spectrum has been neglected. This is a reasonable simplification, since this part of the FAD molecule does not take part in the redox reaction and thus should not contribute significantly to the IR difference spectrum. Figure 2 shows the calculated IR spectra of oxidized and neutral reduced lumiflavin as positive and negative peaks, respectively, for the spectral region between 1800 and 1100 cm^{-1}.

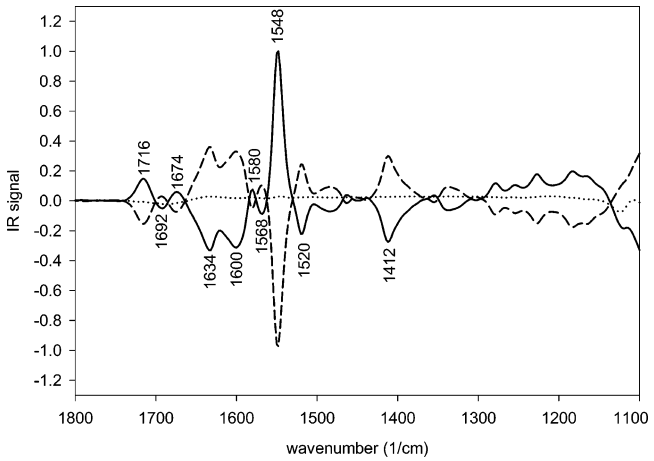

FIGURE 3: Normalized FTIR difference spectra of FAD in 100 mM phosphate buffer (pH 6.0) and 100 mM KCl obtained for potential steps from 0.2 to −0.6 V (vs Ag/AgCl/3 M KCl) (—) and from −0.6 to 0.2 V (– – –). The dotted line is the sum of the two spectra.

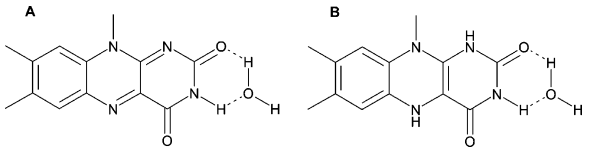

FIGURE 4: Structures of the oxidized (A) and reduced (B) lumiflavin hydrates used for normal-mode analysis.

Interpretation of FAD Difference IR Spectra and Band Assignment. The IR difference spectra of FAD for the redox transition between 0.2 and −0.6 V (vs Ag/AgCl/3 M KCl) in both directions are shown in Figure 3. The dotted line represents the sum of the two spectra. The latter is close to the *x*-axis and devoid of any features, which is an indication that the process is fully reversible. The IR difference spectrum shows a great number of positive and negative peaks, for some of which an assignment to vibrational modes is discussed below. The low noise level can be estimated from the spectral region above 1720 cm^{-1} where no bands are present.

Bands at 1716, 1692, 1674, and 1634 cm^{-1}. It is apparent from a comparison of the plots in Figures 2 and 3 that there is a discrepancy between calculated and measured spectra in the high-frequency region. Aside from approximations intrinsic to the computational method that is used, several other effects must be taken into account. The most important point is that surrounding effects, especially possible hydrogen bonds, are not included in the calculation. The calculated peaks at 1738 cm^{-1} for the oxidized form, which is the sum of two separate bands in proximity (1736 and 1745 cm^{-1}), and at 1766 and 1700 cm^{-1} of the reduced form receive their strongest contribution from C_2═O and C_4═O stretching vibrations, respectively. The carbonyl oxygen is a potential acceptor of hydrogen bonds; hence, these vibrational modes are susceptible to shifts in frequency and intensity upon solvation of the molecule (*11*, *19*). To approach this problem, we considered a system with one water molecule. Starting from a lumiflavin moiety with a single hydrogen bond between C_2═O and water, computational energy minimization surprisingly yielded the structures shown in Figure 4, with a second hydrogen bond formed with the N_3−H group. Normal-mode analysis shows that this hydration already

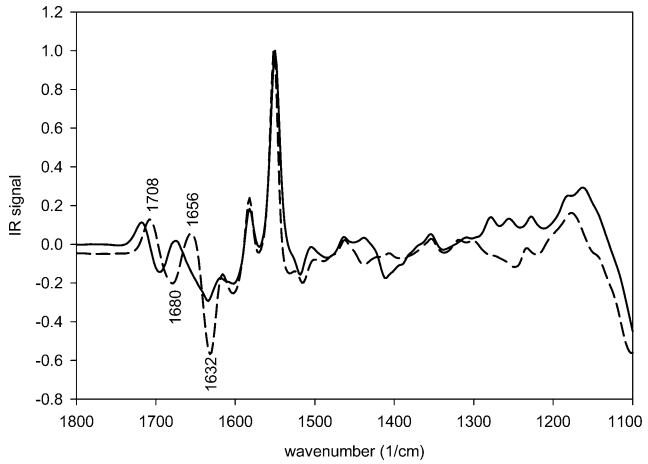

FIGURE 5: Normalized FTIR difference spectra of FAD in 100 mM phosphate buffer in H_2O (—) and D_2O (– – –) at pH/pD 6.0 and 100 mM KCl obtained for a potential step from 0.2 to −0.6 V (vs Ag/AgCl/3 M KCl). The labels refer to the spectrum measured in D_2O.

Table 1: Wavenumbers (in cm^{-1}) of Lumiflavin ν(C═O) Vibrational Modes as a Function of Hydration (Figure 4) and Deuterium Labeling in All Solvent Exchangeable Hydrogen Positions[a]

	^{1}H not hydrated	^{2}H not hydrated	^{1}H hydrated	^{2}H hydrated
oxidized				
$\nu(C_4{=}O)$	1745	1744	1744	1738
$\nu(C_2{=}O)$	1736	1724	1695	1673
reduced				
$\nu(C_4{=}O)$	1700	1690	1702	1684
$\nu(C_2{=}O)$	1766	1753	1724	1706

[a] Hydrogen atoms bound to nitrogen and, in the hydrated forms, the hydrogen atoms of the water molecule itself.

effects a frequency downshift of ∼40 cm^{-1} for the peaks associated with the C_2═O stretch vibration and thus in the direction of the measured peaks. The assignment for the measured bands at 1716, 1692, 1674, and 1634 cm^{-1} to C═O stretch vibrations is further corroborated by a difference spectrum taken from a solution of FAD in D_2O. Here, as reported previously by Hellwig et al. (*14*), these bands are downshifted to 1708, 1680, 1656, and 1632 cm^{-1}, respectively, confirming their dependence on the solvent (Figure 5). Previous results by Nishina et al. demonstrated the assignment of a Raman band at 1711 cm^{-1} of oxidized FAD to a C_4═O mode using an ^{18}O-labeled compound (*8*). Although our normal-mode calculation for reduced lumiflavin is without such supporting precedence, it seems justified to assign the two modes with the highest frequency to the carbonyl stretch modes as well.

Table 1 shows a summary of the calculated frequencies of characteristic bands for both redox states of lumiflavin under a variety of conditions. The trend of decreasing ν(C═O) frequencies upon deuteration or hydration agrees well with the observation, but it is also clear that more aspects of a real solvated state, such as simultaneous hydration of N_1, N_5, and the C_4═O−N_3−H group, would have to be taken into account to obtain more accurate numbers. Final confirmation, however, rests with experiments using isotopically labeled compounds, most importantly in the $C_2{=}^{18}O$ and $C_4{=}^{18}O$ positions.

Bands at 1580 and 1548 cm^{-1}. These prominent bands most likely originate from the $N_5-C_{4a}-C_{10a}-N_1$ region of lumiflavin, where the redox reaction with its rearrangement of single and double bonds and the addition of hydrogen takes place. The calculated bands at 1576 and 1538 cm^{-1} of the oxidized form correspond very well to bands measured at 1580 and 1548 cm^{-1} and represent predominantly $C_{4a}=N_5$ and $C_{10a}=N_1$ stretch modes, respectively. This is in good agreement with previous normal-mode calculations (*10*, *11*). The question of why the intensities of both bands are inverted with respect to the calculated modes arises. Part of the deviation is due to intrinsic shortcomings of the computational method. Another problem, pertaining particularly to the intensities, once again results from the lack of solvent in the calculation. IR band intensities depend on the transition dipole of the vibration. If water as a polar solvent is not arranged perfectly isotropically around the solute, as is likely to be the case due to hydrogen bonding interactions, different modes would experience a different external field and thus a different effect of solvent on intensity. Abe et al. (*20*) have recorded IR spectra of lumiflavin in KBr disks, and these spectra show two peaks of the same height at 1583 and 1552 cm^{-1}. Finally, an additional source of error intrinsic to difference FTIR lies in the subtraction of two spectra. Thereby, apparent peak intensities of the oxidized form are influenced by spectral contributions of the reduced form, and vice versa. It is thus possible that the bands at 1580 cm^{-1} of the oxidized form and at 1600 cm^{-1} of the reduced form partially cancel each other out in the subtraction process and would each show higher intensity in single spectra.

Band at 1600 cm^{-1}. Nishina et al. (*8*) have studied a number of charge transfer complexes of DAO with its amino acid substrates, which contain the reduced form of FAD. These studies involved 4,10a-$^{13}C_2$-labeled FAD and lead to the conclusion that at least in the DAO charge transfer complex a Raman band around 1605 cm^{-1} corresponds to the $C_{4a}=C_{10a}$ stretch mode. Our normal-mode analysis of the reduced form gives a frequency of a similar mode of 1652 cm^{-1}. The theoretical mode contains virtually no contributions from coupled $C_4=O$ stretch vibrations, which agrees very well with its insensitivity to 4-carbonyl ^{18}O labeling (*8*), and our observation that it does not shift in D_2O.

Band at 1520 cm^{-1}. This band most likely corresponds to the calculated feature at 1500 cm^{-1}, which is the sum of two bands in proximity at 1504 and 1497 cm^{-1}. Both result from hydrogen in-plane bending motions. C_6-H and C_9-H bonds contribute to the former mode and N_5-H and N_1-H bonds to the latter, making it thus susceptible to deuteration. Interestingly, there is no pronounced band shift observed in the spectrum measured in D_2O, which would be expected if the assignment is correct. From the frequency calculations of deuterated lumiflavin, we can conclude that this shift exists and is in fact so large that the resulting vibration lies outside the observed window. In the deuterated lumiflavin species, the highest frequency of a mode with a significant contribution of N_5-D/N_1-D in-plane bending motions is 1055 cm^{-1}. It is therefore feasible that the band at 1520 cm^{-1} measured in the *deuterated* species of FAD consists only of the C_6-H/C_9-H in-plane bending, as these protons do not exchange with the solvent. Another good example of such a large shift upon deuteration is the scissoring vibration of H_2O at 1666 cm^{-1} and of D_2O at 1216 cm^{-1} that we found during the normal-mode analysis of the lumiflavin hydrates.

Band at 1412 cm^{-1}. It is not clear whether the measured band at 1412 cm^{-1} corresponds to the calculated features at 1442 and 1364 cm^{-1}. However, both these modes contain as a common property significant contributions from the N_5-H in-plane bending vibration, characteristic of the reduced state. The frequency and intensity of this mode are susceptible to perturbations due to solvent effects, particularly hydrogen bonding, which could explain the difference between the measured and calculated frequency. The IR difference spectrum of FAD in D_2O displays a band at a *higher* frequency than in H_2O. An indication of how this apparent contradiction might be explained is given by the normal-mode analysis of the N_1,N_3,N_5-deuterated reduced species. This calculation also gives upshifted peaks (1461 and 1396 cm^{-1}) in the region of interest, but closer analysis reveals that these no longer receive contributions from N_5-H in-plane bending. The apparent upshift in the deuterated species despite the higher mass of the isotope hence would result from decoupling of motions upon isotopic substitution. Since the bands in this frequency range not only shift significantly upon deuteration but also change their composition entirely, we cannot reach an unambiguous conclusion with this technique about whether the theoretical mode at 1442 or 1364 cm^{-1} corresponds to the observed peak. The assignment to an N_5-H bending vibration as the common feature of both modes is therefore only tentative.

Bands below 1412 cm^{-1}. There are a great number of small bands to be found below 1400 cm^{-1}, in both the measured and calculated spectra, but an assignment becomes increasingly difficult. Normal-mode analysis indicates that these bands result from highly coupled motions across different parts of the isoalloxazine ring system. Because many of these bands thus contain contributions from vibrations that change upon solvation, the lack of hydrogen bonding in the computational model makes assignments to measured modes increasingly doubtful. A hint of the solvent influence can be obtained from the normal-mode analysis of the lumiflavin monohydrates as described above. This single hydration already causes numerous shifts in frequency and/or intensity of the bands below 1400 cm^{-1}, making an assignment of corresponding bands effectively impossible. Another significant contribution to the IR spectrum in this region results from the buffer. Both phosphate and pyrophosphate ions contribute pH-dependent bands below 1200 cm^{-1}. Since during the redox processes both the flavin and the mixture of mediators change their protonation state, buffer peaks are expected to occur.

The assignments of the measured frequencies to vibrational modes for the oxidized and reduced lumiflavin are summarized in Table 2.

IR Difference Spectrum of POX. Figure 6 shows the IR difference spectrum of POX compared to that of FAD. The spectrum represents only the transition from the oxidized to the reduced state (from 0.2 to −0.6 V vs Ag/AgCl/3 M KCl), but reversibility was confirmed by the fact that the difference spectra for the reverse transition are mirror images of those depicted here (data not shown). While the general shape of the spectrum is similar to that of free FAD, it is immediately apparent that there are also numerous differences in detail, in particular concerning the frequency of some prominent peaks.

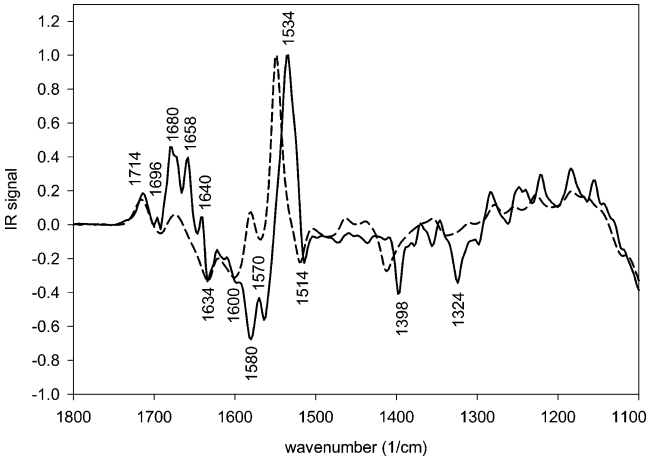

FIGURE 6: Normalized FTIR difference spectra for the potential step from 0.2 to −0.6 V (vs Ag/AgCl/3 M KCl) of pyruvate oxidase in 100 mM phosphate buffer (pH 6.0) and 50 mM KCl (—) and of FAD in 100 mM phosphate buffer (pH 6.0) and 100 mM KCl (− − −). Labels refer to the spectrum of POX.

Table 2: Assignment of Measured Peaks in the Redox-Triggered FTIR Difference Spectrum of FAD to Theoretically Derived Modes of Lumiflavin (Not Hydrated, All ^{1}H Hydrogen Atoms) with Their Major Contributions

measured wavenumber (cm^{-1})	significant contributions	calculated wavenumber (cm^{-1})
oxidized		
1716	$\nu(C_4{=}O)$	1745
1674	$\nu(C_2{=}O)$	1736
1580	$\nu(C_{10a}{=}N_1)$, $\nu(C_{4a}{=}N_5)$	1576
1548	$\nu(C_{10a}{=}N_1)$	1538
reduced		
1692	$\nu(C_2{=}O)$	1766
1634	$\nu(C_4{=}O)$	1700
1600	$\nu(C_{4a}{=}C_{10a})$	1652
1520	$\delta(N_5{-}H)$, $\delta(N_1{-}H)$, $\delta(C_6{-}H)$, $\delta(C_9{-}H)$	1504, 1497
1412	$\delta(N_5{-}H)$ (?)	1442, 1364

Remarkable in this respect is the highest peak at 1534 cm^{-1}, which corresponds to a downshift of ∼14 cm^{-1} in comparison to that of free FAD. If, in a simplified manner, the vibrational band is treated as those it is being caused by a harmonic oscillator, and thus obeys $f = \sqrt{k/m_r}/(2\pi)$ (f is the frequency, k the force constant, and m_r the reduced mass), a decrease in frequency of 0.9% is caused by a 1.8% decrease in the force constant, corresponding to a weakening of the vibrating bonds. A similar downshift can be seen for the peak at 1580 cm^{-1} in free FAD, which appears at 1570 cm^{-1} in the protein-bound species. Since the modes at 1580 and 1548 cm^{-1} receive their greatest contribution from $C_{4a}{=}N_5$ and $C_{10a}{=}N_1$ stretch vibrations, a loosening of these bonds would shift the structure of the molecule toward the reduced form, where these two are single bonds. Interestingly, this corresponds to the observation that the isoalloxazine moiety of POX-bound FAD is bent along the $N_5{-}N_{10}$ axis, resembling the conformation of reduced FAD. It is therefore possible that the distortion of FAD as observed in the crystal structure causes the peak shifts in the IR spectrum. The peak at 1534 cm^{-1} also shows a shoulder at ∼1522 cm^{-1} that is not visible in the spectrum of FAD, but its assignment is not clear. Interestingly, the band at 1600 cm^{-1}, attributed to the $C_{4a}{=}C_{10a}$ stretch vibration of the reduced state, remains unchanged in the protein-bound cofactor.

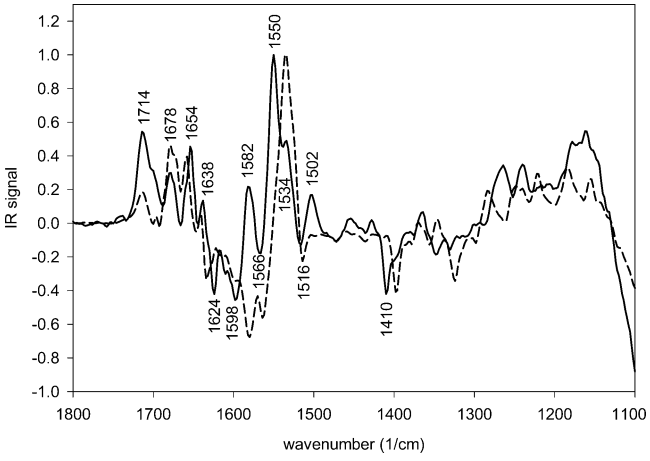

FIGURE 7: Normalized FTIR difference spectra for the potential step from 0.2 to −0.6 V (vs Ag/AgCl/3 M KCl) of glucose oxidase in 100 mM phosphate buffer (pH 6.5) and 100 mM KCl (—) and of pyruvate oxidase in 100 mM phosphate buffer (pH 6.0) and 50 mM KCl (− − −). Labels refer to the spectrum of GOX.

Between 1500 and 1700 cm^{-1}, spectral contributions of the protein would be expected, since this is the region of the backbone amide bands. Indeed, the POX difference spectrum contains some features that are not present in the FAD spectrum. However, it is not possible at present to assign these bands to specific modes of the protein near the cofactor. A meaningful theoretical modeling by far exceeds the available computational resources at the moment, and a crystal structure of the reduced enzyme, which would be helpful for the interpretation, is not available.

The band at 1714 cm^{-1}, the only carbonyl stretch band not obscured by contributions from the protein, remains almost unchanged upon binding of FAD to the protein, indicating that the hydrogen bonding strength at this carbonyl group ($C_4{=}O$) is similar in the bound state and in solution.

There are two more prominent peaks of the reduced state at 1324 and 1398 cm^{-1}. The origin of the former is ambiguous, but the latter is probably equivalent to the FAD band at 1412 cm^{-1}. This would constitute another example of a large frequency shift in the spectrum of FAD upon binding to the protein, most likely caused by a difference in hydrogen bonding at the $N_5{-}H$ group in the bound state versus in solution.

As a control experiment, a difference spectrum of the apoenzyme without the bound cofactor was measured. As expected, the spectrum was identical to that of buffer alone (data not shown). This indicates that all redox-induced differences in the spectra, including those of the protein, depend on the presence of the redox active cofactor FAD.

IR Difference Spectra of GOX and DAO. FTIR difference spectra of GOX and DAO in comparison to that of POX are given in Figures 7 and 8, respectively.

IR Difference Spectrum of GOX. The IR difference spectrum of glucose oxidase (Figure 7) also exhibits a number of peaks that derive from the flavin cofactor, but it is considerably different from the spectrum of POX. The two peaks of FAD at 1548 and 1580 cm^{-1}, which are downshifted in the spectrum of POX, are upshifted, albeit slightly, in GOX toward 1550 and 1582 cm^{-1}, respectively. A small peak at 1534 cm^{-1} might correspond to the shoulder of the peak at 1534 cm^{-1} in POX, but again its assignment is ambiguous. Since the available crystal structure of the

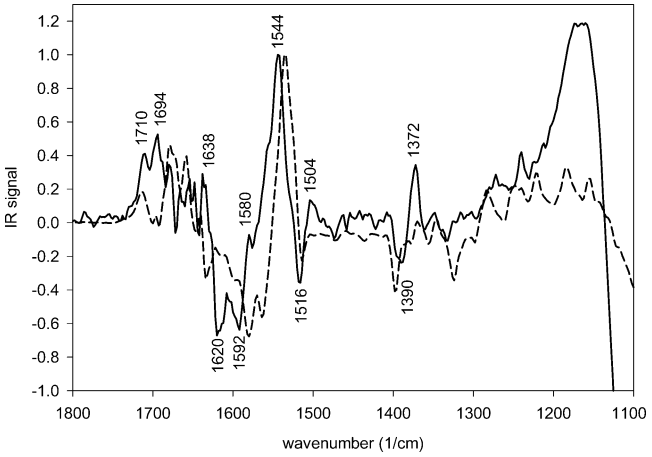

FIGURE 8: Normalized FTIR difference spectra for the potential step from 0.2 to −0.6 V (vs Ag/AgCl/3 M KCl) of D-amino acid oxidase in 100 mM pyrophosphate buffer (pH 8.3) 100 mM KCl (—) and of pyruvate oxidase in 100 mM phosphate buffer (pH 6.0) and 50 mM KCl (— — —). Labels refer to the spectrum of DAO.

GOX enzyme at a resolution of 1.9 Å [PDB entry 1CF3 (*21*)] gives no indication of a bend in the isoalloxazine ring, the fact that the IR peaks are hardly shifted corroborates the assumption that the peak shift in POX is caused by the distortion of the cofactor. Similarly, the peak at 1412 cm^{-1} in FAD (1398 cm^{-1} in POX) is only slightly shifted to 1410 cm^{-1} in GOX. On the other hand, the band corresponding to the C_4═O stretch vibration of the reduced cofactor, found at 1634 cm^{-1} in FAD and POX, is shifted toward 1624 cm^{-1} in GOX.

The highest-wavelength band, as in FAD (1716 cm^{-1}) and POX (1714 cm^{-1}), is the C═O stretch mode at 1714 cm^{-1}, although its intensity in GOX is higher. As in POX, the region between 1700 and 1500 cm^{-1} exhibits many additional peaks resulting from the protein environment of the cofactor, which so far cannot be attributed to specific modes. Haouz et al. (*22*) report a shape analysis of the GOX amide I′ band depending on the oxidation state of the enzyme, but they discuss the resulting differences in the composition of the bands between 1600 and 1700 cm^{-1} only in terms of varying contributions from secondary structure elements of the protein alone. In light of the study presented here, this interpretation appears to be incomplete, as the similarity of the IR difference spectra of FAD and GOX argues for a much stronger contribution of the cofactor in this spectral region.

IR Difference Spectrum of DAO. The signal-to-noise ratio of the DAO IR difference spectrum (Figure 8) is lower than in the previous spectra, as judged from the baseline above 1720 cm^{-1}; therefore, a discussion of the fine structure of the spectrum is not appropriate. The large differences between POX and DAO in the region from 1200 to 1100 cm^{-1} result from the use of a pyrophosphate as the buffering ion in the case of DAO. Despite these limitations, some prominent features derived from the bound cofactor FAD are clearly visible. In particular, a significant peak at 1544 cm^{-1}, associated with C_{10a}═N_1 stretch vibrations, is visible for this protein as well. This corresponds to a slight downshift of 4 cm^{-1} compared to that of free FAD and thus in the same direction as in POX, albeit to a lesser extent. The best available crystal structure of porcine kidney DAO [PDB entry 1AA8 (*23*)] with a resolution of 2.5 Å indicates a slight bend of ∼6° along the N_5−N_{10} axis in the isoalloxazine moiety, supporting the interpretation of the peak shift as being caused by steric strain.

CONCLUSIONS

A comparison of the redox-triggered FTIR difference spectra of FAD and the three flavoproteins (POX, GOX, and DAO) indicates that despite numerous differences in detail the protein spectra have an overall shape similar to the shape of the spectrum of FAD, arguing that the enzymes do not undergo a significant rearrangement in their secondary or tertiary structure upon a change in redox state. Several prominent peaks in the FTIR difference spectra can be assigned to distinct vibrational modes of FAD based on DFT frequency calculations, and for the first time, an attempt was made to extend this band assignment to the reduced form of the flavin. The differences in position and intensity of some peaks between the free and bound form of the cofactor may provide insight into the mode of binding of the cofactor. Zheng et al. have described a Raman spectroscopy study with *p*-hydroxybenzoate hydroxylase, where they could discern a solvent-exposed and a buried binding mode of the cofactor FAD (*24*). In the study presented here, we observed a unique ∼14 cm^{-1} shift of two peaks assigned to C_{10a}═N_1 and C_{4a}═N_5 stretch vibrations of FAD upon binding to pyruvate oxidase. Although similar peaks have been observed in previous resonance Raman studies of other flavoenzymes, in no instance have such large shifts been reported. We propose that these shifts reflect the strained conformation of the cofactor that has been observed in the crystal structure (*6*).

The bent conformation of the flavin cofactor in POX which resembles its reduced state suggests an elevated redox potential of the FAD bound to the protein versus free in solution. Indeed, a stepwise potentiometric titration in the IR cell yields a midpoint potential of POX which is 75 mV higher than that of the free cofactor under the same conditions (−300 and −375 mV vs Ag/AgCl/3 M KCl, respectively; curves not shown). However, in DAO the FAD is not bent to the same extent, yet here the redox potential of the bound FAD also is up to 180 mV higher than in the free form (depending on the pH; see ref *25*); a similar argument can be made for GOX (*26*). Clearly, besides the conformation of the cofactor, its environment in the enzyme, in particular hydrogen bonding and electrostatic interactions, influences its redox properties. To separate these from conformational effects, we are now investigating a variant of POX with an amino acid exchange in the isoalloxazine binding pocket (Val^{265}Ala).

With respect to line widths, one might expect a narrowing of those bands that are influenced by solvation upon binding of FAD to the protein, reflecting the more homogeneous environment of the cofactor when bound to protein versus in solution. From the measured spectra, this is somewhat difficult to ascertain, mostly because of the overlapping of bands from oxidized and reduced states in the difference spectra. However, as far as the peaks in the crowded region of the POX and GOX spectra between 1700 and 1600 cm^{-1} can be separated, they appear to be sharper than those in the spectrum of FAD. The bands at 1398 cm^{-1} of POX and at 1410 cm^{-1} of GOX are also narrower than their equivalent at 1412 cm^{-1} of free FAD. On the other hand, the carbonyl

bands at 1714 cm^{-1} have a similar shape in all three spectra. (The DAO spectrum shows too much noise to be included in this discussion.) In summary, the narrowing of solvent-dependent lines is difficult to quantify, but cannot be ruled out.

As the results presented here show, redox-triggered FTIR spectroscopy can be applied successfully to the study of flavoproteins. The method complements other techniques of vibrational spectroscopy; the FTIR difference spectra contain information pertaining to a chemical process relevant for catalysis, and they provide a way to study the reduced form of FAD, which is difficult with resonance Raman spectroscopy. Although several resonance Raman studies have been carried out with charge transfer complexes of reduced flavoproteins and their substrates or substrate analogues [D-amino acid oxidase (*27*), acyl-CoA dehydrogenase (*28*), and L-phenylalanine oxidase (*29*)], aside from one peak observed around 1600 cm^{-1} all other peaks in these spectra have been attributed to the respective ligand rather than the flavin cofactor. The FTIR difference spectra, on the other hand, contain a large number of features that must be derived from the flavin. However, to use the method to its full potential, further research must be directed at an unambiguous assignment of the observed bands through isotopically labeled flavin derivatives and/or isotopic labeling of the apoenzyme. As long as these are not available, quantum chemical calculations can provide helpful information, as demonstrated here.

ACKNOWLEDGMENT

We thank Prof. R. Jaenicke and Mrs. A. Jaenicke for their generous support, Dr. P. Hellwig for helpful discussions, and Mr. J. Fanghänel, Mrs. A. Schütz, and Dr. K. Tittmann for comments on the manuscript.

REFERENCES

1. MacDonald, I. D. (1999) *Methods Mol. Biol. 131*, 125−138.
2. Stanley, R. J. (2001) *Antioxid. Redox Signaling 3*, 847−866.
3. Zheng, Y., Massey, V., Schaller, A., Palfey, B. A., and Carey, P. R. (2001) *J. Raman Spectrosc. 32*, 579−586.
4. Moss, D., Nabedryk, E., Breton, J., and Mäntele, W. (1990) *Eur. J. Biochem. 187*, 565−572.
5. Mäntele, W. (1993) *Trends Biochem. Sci. 18*, 197−202.
6. Muller, Y. A., Schumacher, G., Rudolph, R., and Schulz, G. E. (1994) *J. Mol. Biol. 237*, 315−335.
7. Kitagawa, T., Nishina, Y., Kyogoku, Y., Yamano, T., Ohishi, N., Takai-Suzuki, A., and Yagi, K. (1979) *Biochemistry 18*, 1804−1808.
8. Nishina, Y., Sato, K., Miura, R., Matsui, K., and Shiga, K. (1998) *J. Biochem. 124*, 200−208.
9. Bowman, W. D., and Spiro, T. G. (1981) *Biochemistry 20*, 3313−3318.
10. Abe, M., and Kyogoku, Y. (1987) *Spectrochim. Acta 43A*, 1027−1037.
11. Lively, C. R., and McFarland, J. T. (1990) *J. Phys. Chem. 94*, 3980−3994.
12. Birss, V. I., Hinman, A. S., McGarvey, C. E., and Segal, J. (1994) *Electrochim. Acta 39*, 2449−2454.
13. Sedewitz, B., Schleifer, K.-H., and Götz, F. (1984) *J. Bacteriol. 160*, 273−278.
14. Hellwig, P., Scheide, D., Bungert, S., Mäntele, W., and Friedrich, T. (2000) *Biochemistry 39*, 10884−10891.
15. Frisch, M. J., Trucks, G. W., Schlegel, H. B., Scuseria, G. E., Robb, M. A., Cheeseman, J. R., Zakrzewski, V. G., Montgomery, J. A., Jr., Stratmann, R. E., Burant, J. C., Dapprich, S., Millam, J. M., Daniels, A. D., Kudin, K. N., Strain, M. C., Farkas, O., Tomasi, J., Barone, V., Cossi, M., Cammi, R., et al. (1998) *Gaussian 98*, revision A.3, Gaussian, Pittsburgh, PA.
16. Scott, A. P., and Radom, L. (1996) *J. Phys. Chem. 100*, 16502−16513.
17. Zheng, Y., and Ornstein, R. L. (1996) *J. Am. Chem. Soc. 118*, 9402−9408.
18. Rizzo, C. J. (2001) *Antioxid. Redox Signaling 3*, 737−746.
19. Hazekawa, I., Nishina, Y., Sato, K., Shichiri, M., Miura, R., and Shiga, K. (1997) *J. Biochem. 121*, 1147−1154.
20. Abe, M., Kyogoku, Y., and Kitagawa, T. (1986) *Spectrochim. Acta 42A*, 1059−1068.
21. Wohlfahrt, G., Witt, S., Hendle, J., Schomburg, D., Kalisz, H. M., and Hecht, H. J. (1999) *Acta Crystallogr. D55*, 969−977.
22. Haouz, A., Twist, C., Zentz, C., Tauc, P., and Alpert, B. (1998) *Eur. Biophys. J. 27*, 19−25.
23. Mizutani, H., Miyahara, I., Hirotsu, K., Nishina, Y., Shiga, K., Setoyama, C., and Miura, R. (1996) *J. Biochem. 120*, 14−17.
24. Zheng, Y., Dong, J., Palfey, B. A., and Carey, P. R. (1999) *Biochemistry 38*, 16727−16732.
25. Brunori, M., Rotilio, G. C., and Antonini, E. (1970) *J. Biol. Chem. 246*, 3140−3144.
26. Stankovich, M. T., Schopfer, L. M., and Massey, V. (1978) *J. Biol. Chem. 253*, 4971−4979.
27. Nishina, Y., Shiga, K., Miura, R., Tojo, H., Ohta, M., Miyake, Y., Yamano, T., and Watari, H. (1983) *J. Biochem. 94*, 1979−1990.
28. Nishina, Y., Sato, K., Hazekawa, I., and Shiga, K. (1995) *J. Biochem. 117*, 800−808.
29. Suzuki, H., Koyama, H., Nishina, Y., Sato, K., and Shiga, K. (1991) *J. Biochem. 110*, 169−172.

BI035219F